

case of perturbations of the temperature field due to the side walls, as occurs in practice, and, in particular, in the necks of vessels containing liquid nitrogen, the free-convective heat transfer of free convection can be evaluated by using the curve shown in Fig. 2.

NOTATION

ϵ_c , free convection coefficient; D, neck diameter; L, height of the neck; Ra, Rayleigh number; Nu, Nusselt number; Pr, Prandtl number.

LITERATURE CITED

1. B. M. Berkovskii and V. E. Fertman, Heat and Mass Transfer [in Russian], Vol. 1, Part 3, Minsk (1972), p. 249.
2. A. V. Lykov, Heat and Mass Transfer, Handbook [in Russian], Énergiya, Moscow (1972).
3. V. E. Fertman, in: Energy Transfer in Channels, Énergiya, Moscow (1970), p. 179.
4. A. V. Lykov, B. M. Berkovskii, and V. E. Fertman, Inzh.-Fiz. Zh., 16, No. 6 (1969).
5. S. P. Gorbachev, Inzh.-Fiz. Zh., 15, No. 1, 40 (1968).
6. S. P. Gorbachev and M. G. Kaganer, Tr. Vses. Nauchno-Issled. Inst. Kriog. Mashinostr., No. 13, 68 (1971).
7. M. G. Kaganer, Tr. NPO Kriog. Mashinostr., No. 15, 174 (1973).
8. E. M. Sparrow, Advances in Heat Transfer, Part 2, Academic Press, New York-London (1965), p. 465.
9. V. P. Isachenko, A. S. Sukomel, and V. A. Osipova, Heat Transfer [in Russian], Énergiya, Moscow (1969).

NUMERICAL INVESTIGATION OF LIGHT-ABSORBENT CONVECTION IN HORIZONTAL TUBE

I. STEADY CONVECTION STATES IN THE FIELD OF CONTINUOUS LASER RADIATION

B. P. Gerasimov, V. M. Gordienko,
and A. P. Sukhorukov

UDC 536.25

The dependence of the rate of steady photoabsorptive convection in liquids, gases, and plasmas on the intensity of a horizontal laser beams is studied. A good agreement with the results of dimensional analysis is obtained.

1. Introduction

The propagation of laser radiation in an absorbing medium results in the latter being heated. The arising temperature gradients lead to the development of the convective motions in liquids or gases; the study of the latter was the subject of a considerable number of articles both experimental and theoretical character [1-6].

Since the Navier-Stokes equations governing the convection are nonlinear, analytical methods yield only some general laws, and a detailed study of convective motion is only feasible by employing numerical methods.

In [7-9] numerical simulation was carried out of photoabsorptive convection in a chamber which is uniformly irradiated orthogonally to the lengthwise axis of the chamber. In the present article numerical investigation is carried out on convective motion in liquid, gases, or plasma which arises in a long horizontal vessel of rectangular cross section exposed to a laser beam of small diameter traveling along its axis. The problem had previously been considered by us using the dimension theory [6]. It predicted the existence of three states of

Institute of Applied Mathematics, Academy of Sciences of the USSR, Moscow. M. V. Lomonosov Moscow State University, Moscow. Translated from Inzhenerno-Fizicheskii Zhurnal Vol. 33, No. 4, pp. 709-718, October, 1977. Original article submitted June 12, 1975.

photoabsorptive convection depending on the magnitude of the dimensionless parameter of heat emission q , which is proportional to the intensity of the laser beam.

The characteristic velocity of convective motion due to laser heating is given by the relation $V = C(\text{Pr})q^N$ where the convection constant $C(\text{Pr})$ and the convection exponent N , ($N = 1/2, 1/3$) are modified with the growth of q in the transition from one state to another.

In the present article this relation is obtained by numerically solving the complete system of Navier–Stokes equations in their Boussinesq approximation. The values of the convection constants $C(\text{Pr})$ are determined, which cannot be done by using the similarity concepts; also determined is their dependence on the geometrical factor L/α , the ratio of the chamber linear dimension L to the radius α of the laser beam. The latter enables one to specify more accurately the bounds for the existence of these states. The temperature field and the velocity field of a steady convective motion have their own special qualitative features for each of the three states. It is characteristic that in the numerical experiments for large values of the heat-emission parameter $q \approx 10^9$ a large number of secondary vortices appear, which points to the possibility of turbulence of the convective flow in the case of steady heating by radiation of this intensity.

In the second part of the article the results will be given of a numerical investigation of the procedure of setting up in time of convective flows and temperature.

2. Formulation of the Problem

The convective motion due to the absorption of laser radiation in an elongated vessel of rectangular section, the radiation being propagated parallel to the vessel axis (z axis), is obtained experimentally. With flow velocities much lower than the sound velocity in this medium and with small vertical dimension H of the flow region ($H \ll RT/\mu g$) the gas density changes only slightly and the heat dissipation is slight. The compression work can, therefore, be neglected and the density can be regarded as constant with the exception of the contribution of density changing into buoyancy force. In this case the motion of a viscous and heat-conducting gas (liquid) is governed by the system of the Navier–Stokes equations in the Boussinesq approximation [6]:

$$\begin{aligned} \frac{\partial \vec{V}}{\partial t} + (\vec{V}\nabla)\vec{V} &= -\frac{1}{\rho_0}\nabla p + \nu\Delta\vec{V} + \beta\vec{g}(T - T_0), \\ \frac{\partial T}{\partial t} + (\vec{V}\nabla)T &= \chi\Delta T + \frac{\alpha I_0 e^{-\alpha z}}{\rho_0 c_p} f(r/\alpha), \quad \text{div}\vec{V} = 0, \end{aligned} \quad (1)$$

where $p = P - \rho_0(\vec{g}\vec{r})$ is the Boussinesq quasipressure; $f(r/\alpha)$ is a function which characterizes the intensity profile of the laser beam of radius α .

In carrying out the computations it was assumed that the vessel length exceeds many times its cross section; thus, the effect of the ends is small and the heating by laser radiation is uniform along the axis (this takes place if a small part of the beam energy is absorbed, $\alpha z \ll 1$). Under these assumptions and by taking into account that the velocity along the vessel axis is assumed to vanish our problem becomes two-dimensional.

By introducing the stream function ψ such that $V_x = \partial\psi/\partial y$, $V_y = -\partial\psi/\partial x$, and $\vec{\omega} = \text{rot}\vec{V} = (0, 0, \omega)$ Eqs. (1) become more suitable for numerical work after their dimensionless quantities have been introduced:

$$\begin{aligned} \frac{\partial \omega}{\partial t} + \frac{\partial}{\partial x} \left(\frac{\partial \psi}{\partial y} \omega \right) - \frac{\partial}{\partial y} \left(\frac{\partial \psi}{\partial x} \omega \right) &= \Delta \omega + \frac{\partial T}{\partial x}, \\ \frac{\partial T}{\partial t} + \frac{\partial}{\partial x} \left(\frac{\partial \psi}{\partial y} T \right) - \frac{\partial}{\partial y} \left(\frac{\partial \psi}{\partial x} T \right) &= \frac{1}{\text{Pr}} \Delta T + qf(x, y), \quad \omega = -\Delta\psi. \end{aligned} \quad (2)$$

The dimensionless quantities in (2) and in our further considerations are denoted by the same letters as the corresponding dimensional ones and to avoid confusion a tilde is put over them.

We adopted as independent dimensions L , the width of the vessel, ν and β ; the dimensional and dimensionless quantities are related by the following:

$$\tilde{r} = r/L; \quad \tilde{x} = x/L; \quad \tilde{y} = y/L; \quad \tilde{t} = t\nu/L^2; \quad \tilde{\omega} = L^2\omega/\nu;$$

Using a 21 x 21 grid the computations were carried out by the implicit finite-difference method described in [10] with the following values of the parameters: $10 \leq q \leq 10^8$, $Pr = 1, 20, 0.05$; $a/L = 0.1, 0.05, 0.025$; $H/L = 1, 2$. To check the error, sample checking calculations were carried out on a 41×41 grid; they show that the 21×21 grid yields sufficiently good results (the discrepancy did not exceed a few percentages).

$$(4) \quad f(x, y) = \exp \left(- \frac{a^2}{(x - L/2)^2 + (y - L/2)^2} \right)$$

the wall temperature is kept constant: $T = T_0$. The profile of the laser beam is assumed to be Gaussian:

$$\psi = \frac{\partial \phi}{\partial x} = \frac{\partial \psi}{\partial y} = 0;$$

field:

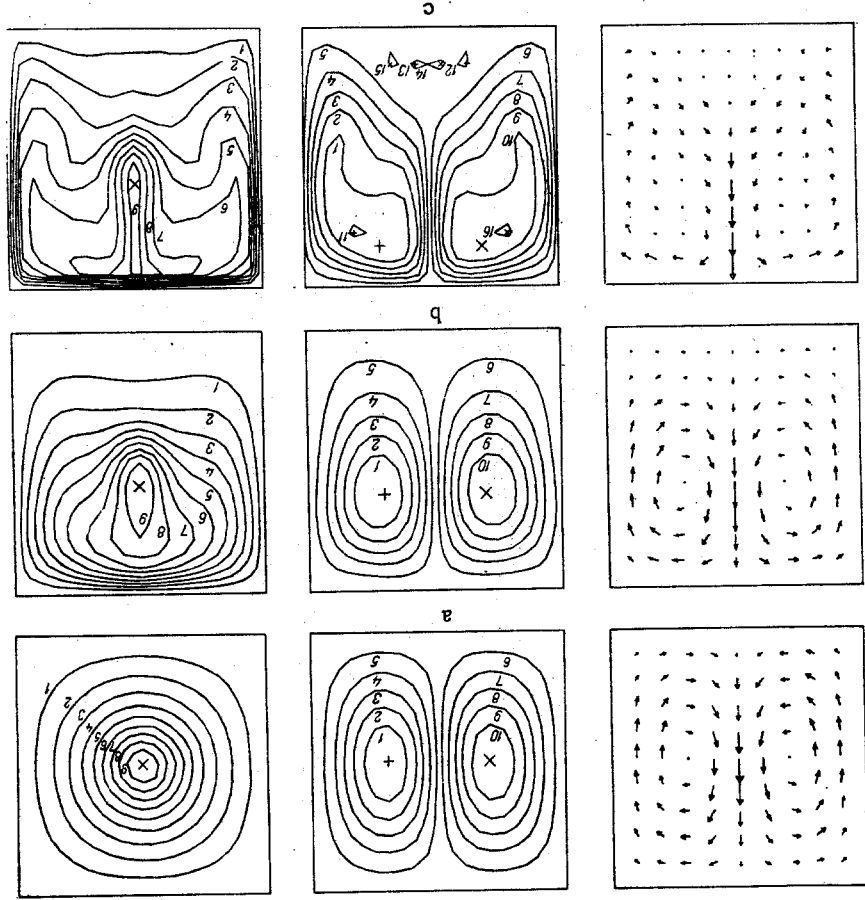
On the vessel walls the boundary conditions of adhesion and no leaking must be satis-

$$(3) \quad \bar{q} = \left(\frac{a}{L} \right)^2 q_{Re}; \quad \bar{V} = \frac{a}{L} V_{Re}; \quad \bar{T} = \left(\frac{a}{L} \right)^3 T_{Re}$$

If instead of L the beam radius a is adopted for the space dimension, then the variables ob-

$$\bar{T} = | \beta g (T - T_0) L^3 / a^2; \quad \bar{q} = (\alpha L^3 \beta g) / (\rho c^2 a^3); \quad \bar{V} = LV/a; \quad \bar{\psi} = \psi/a.$$

Fig. 1. Map of gas convection (Pr = 1) in a horizontal square tube (H = L) in a laser-beam field with $a = 0.1L$. From left to right: velocity field \bar{V} , streamlines $\psi = \text{const}$, isotherms $\bar{T} = \text{const}$; a) $q = 10^2$; $\psi^* = -\psi^+ = 4.54 \cdot 10^{-4}$; $\bar{T}^* = 10^2$; b) $q = 10^7$; $\psi^* = -\psi^+ = 8.57$; $\bar{T}^* = 3.11 \cdot 10^4$; c) $q = 10^8$; $\psi^* = -\psi^+ = 3.48 \cdot 10^2$; $\bar{T}^* = 0.00$; $\psi_{12} = -\psi_{12} = 0.01$; $\psi_{16} = -\psi_{11} = 3.40$; $\bar{T}^* = 1.07 \cdot 10^6$.



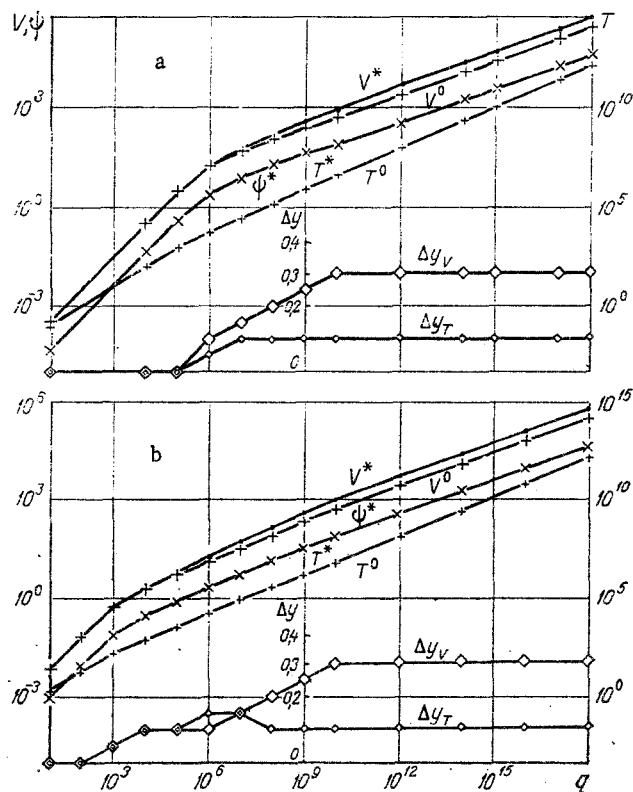


Fig. 2. Principal parameters of photoabsorptive convection versus heat release q : a) $Pr = 1$; $\alpha/L = 0.1$; $H/L = 1$; b) $Pr = 20$; $\alpha/L = 0.1$; $H/L = 1$.

3. Steady Convective Motion

The steady-state solution of the equations was found by the adjustment method. At the initial state the fluid velocity in the vessel is zero and the temperature is uniform: $T = T_0$.

In Fig. 1 the field velocities, the isotherms, and the streamlines are shown for the three characteristic values of q .

The arrow lengths on the map of the velocity field are proportional to the velocity vectors, the scaling proportionality coefficient being selected for each graph so that the arrows do not intersect.

The values of the level lines for ψ and T are selected automatically, the basic level lines being equidistant:

$$\psi_n = \psi^+ + \frac{\psi^* - \psi^+}{11} n \quad (n = 1, \dots, 10); \quad T_n = \frac{T^*}{10} n \quad (n = 1, \dots, 9).$$

The bigger crosses show the maximum (\times) or the minimum ($+$) of a function, and the smaller crosses the local maxima or minima which can be seen from the additional level lines ($n = 11-16$).

In Fig. 2 some characteristic parameters of convection are shown in the logarithmic scale versus the heat release q . The marks on the curves show these values of q for which computations have been carried out.

The larger or smaller marks $+$ show the curves of velocity V^0 or of temperature T^0 , respectively, on the laser beam axis, and the curves which adjoin them closely above correspond to the maximal values of velocity or temperature in the flow field V^* , T^* . The displacement graphs of the velocity Δy_V or temperature Δy_T maxima relative to the beam axis are shown by large or small squares both given in the ordinary scale. The mark \times shows the maximum of the stream function ψ^* which characterizes the amount of fluid from the beam in a unit of time.

TABLE 1

Pr	a/L	C ₁	C ₂	C ₃
1	0,1	3,5·10 ⁻⁵	missing	0,46
1	0,05	1,1·10 ⁻⁵	missing	0,46
20	0,1	7,2·10 ⁻⁴	3·10 ⁻²	0,46
0,05	0,1	1,7·10 ⁻⁶	not available	0,46

3.1. Weak Convection. To the state of weak convection in Fig. 2 there corresponds an initial region of q values for which the following linear relation holds:

$$V = C_1(\text{Pr})q, \quad (5)$$

where V is the characteristic convection rate. The convection constant $C_1(\text{Pr})$ obtained by means of numerical experiments in the range $10^{-2} \leq \text{Pr} \leq 10^4$ has proved to be directly proportional to the Prandtl number (Table 1). It is also noticed that if the beam radius is adopted for the scale length $V_{\text{Re}} = \bar{C}_1 q_{\text{Re}}$, then $\bar{C}_1(\text{Pr}) = C_1(L/a)^4 \approx \text{Pr}$. The upper bound of this state for $\text{Pr} = 20$ is given by $q \approx 10^2$ - 10^3 ; for $\text{Pr} = 1$ it is $q \approx 10^5$; for $\text{Pr} = 0.05$ it is $q \approx 10^7$, which is in good agreement with the results of the dimensional analysis in [6] (for a thin ray with $a/L = 0.5$ for $\text{Pr} = 1$ the limit of the state is $q \approx 10^6$; however, the lowering of the beam radius has to be taken into account and this introduces a multiplier of 2^{-4}). Numerical experiments have shown that in the weak-convection state the structure of convective motion is virtually independent of Pr , q , or L/H , and only its intensity varies. The isotherms are almost circular in this state (see Fig. 1). This indicates that the velocity field exerts no effect on the heat dissipation from the zone of heat release, which is a particularly distinctive feature of this state, as noted in [6].

The problem of weak convection in a circular cylinder of radius R was solved in [11] with the aid of the following equations:

$$\nabla^2 T = -q \text{Pr} \exp(-r^2/a^2), \quad (6)$$

$$\nabla^4 \psi = \frac{\partial T}{\partial r} \cos \varphi \quad (7)$$

(where r and φ are polar c-ordinates), which can be obtained from Eqs. (2) by making the left-hand sides vanish. The respective solutions are given by [see Eq. (3)]

$$T_{\text{Re}} = \frac{q_{\text{Re}} \text{Pr}}{4} \left[\text{Ei} \left(-\frac{r^2}{a^2} \right) - 2 \ln \frac{r}{R} - \text{Ei} \left(-\frac{R^2}{a^2} \right) \right], \quad (8)$$

$$\begin{aligned} \psi = & \frac{q_{\text{Re}} \text{Pr}}{4} \left\{ \left(\frac{r}{a} + \frac{1}{3} \frac{r^3}{a^3} \right) \left[\text{Ei} \left(-\frac{r^2}{a^2} \right) - 2 \ln \frac{r}{R} \right] + \right. \\ & \left. + \frac{\left(1 + \frac{r^2}{a^2} \right) \exp \left(-\frac{r^2}{a^2} \right) - 1}{2r/a} + A_1 \frac{r}{a} + A_2 \frac{r^3}{a^3} \right\} \cos \varphi, \quad (9) \end{aligned}$$

where

$$A_1 = \left[2 \ln \left(\frac{R}{a} \right) - \text{Ei} \left(-\frac{R^2}{a^2} \right) \right] + \frac{1 - \exp \left(-\frac{R^2}{a^2} \right)}{(R/a)^2} - \left(1 + \frac{1}{2} \frac{R^2}{a^2} \right), \quad (10)$$

$$A_2 = \frac{1}{2} \left[2 \ln \left(\frac{R}{a} \right) - \text{Ei} \left(-\frac{R^2}{a^2} \right) \right] + \frac{\left(1 - \frac{R^2}{a^2} \right) \exp \left(-\frac{R^2}{a^2} \right) - 1}{2 \left(\frac{R}{a} \right)^4} + \frac{a^2}{R^2} + \frac{1}{2}. \quad (11)$$

From the expression (9) for the stream function one can easily obtain the convection rate at the point (r, φ) by employing the relation

$$V_r = \frac{1}{r} \frac{\partial \psi}{\partial \varphi}, \quad V_\varphi = -\frac{\partial \psi}{\partial r}.$$

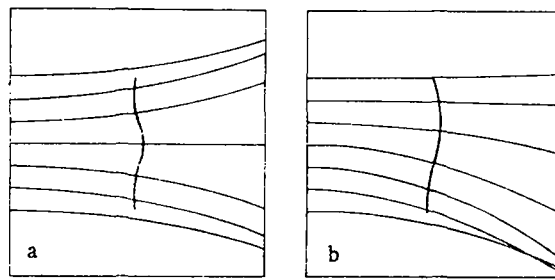


Fig. 3. Beam trajectories in a vessel with light-absorbing convection (convection in vertical plane normal to the diagram): a) weak convection $q = 100$; $Pr = 1$; b) full convection $q = 10^{12}$; $Pr = 1$.

For example, on the beam axis ($r = 0$) one has

$$V_{Rc}^0 = \frac{q_{Re} Pr}{32} \frac{a^2}{R^4} \left[\left\{ Ei \left(-\frac{R^2}{a^2} \right) - 2 \ln \left(\frac{R}{a} \right) \right\} + \left(1 + \frac{R^2}{2a^2} \right) - \frac{1 - \exp(-R^2/a^2)}{(R/a)^2} - 0.5772 \dots \right]; \quad (12)$$

hence it can be seen that for weak convection its rate depends on the ratio of the radius of the vessel and of the beam; this can also be seen in the numerical experiments (see Table 1). By setting $R = L/2$ one obtains from (12) in the case of $R/a \gg 1$ [by employing (3)] that

$$V^0 \approx \frac{q Pr}{256} \frac{a^2}{L^2} \left[1 + \frac{8a^2}{L^2} \left(1 - \ln \frac{L^2}{4a^2} \right) \right]. \quad (13)$$

Substituting in (13) $L/a = 10$ and 20 , $Pr = 1$, one finds for the convection constant the values $C_1 = 4 \cdot 10^{-5}$ and 10^{-5} , which are in good agreement with the results of numerical computations (Table 1).

3.2. Moderate Convection. In accordance with the assessment of [6] the state of moderate convection with the characteristic formula

$$V = C_2(Pr)q^{1/2} \quad (14)$$

can be observed in fluids or plasma with $Pr \neq 1$. In the numerical experiments this state was maintained only for liquids ($Pr = 20$) but it was not observed in media with $Pr \ll 1$ with various values of L/a , H/L , Pr . No explanation could be found for this phenomenon. One could assume that the absence of a relation of the type (14) in the numerical experiments could be related to the effect exerted by the walls [since (14) was obtained for unbounded space] though the calculations with $a/L = 0.025$ on the 41×41 grid did not confirm it; it is likely, however, that an even thinner laser beam might be necessary. It is also possible that the absence of this state could be due to considerable artificial viscosity of the adopted difference scheme. Indeed, according to [6], in the state of moderate convection in plasma the convective terms dominate the viscous terms. Artificial viscosity can disturb this balance. Nevertheless, a negative result on a denser grid casts some doubt since for smaller steps of the grid schematic viscosity becomes lower.

It may prove expedient to employ a scheme with a small artificial viscosity, although these schemes make the computations for large q impossible. For $Pr = 20$ the moderate convection state takes place for the range of the values $10^5 \leq q \leq 10^9$, which agrees with the results of the dimensional analysis [6]. For $Pr = 20$ the coefficient of proportionality is equal to $C_2 = 3 \cdot 10^{-2}$. In this state a progressive distortion of the isotherms takes place due to the velocity field. The maxima of temperature and velocity are displaced upward from the beam center. The displacement of the velocity maximum takes place since the heat is carried away convectively; this results in considerable horizontal gradients of temperature above the beam axis which produce a further fluid acceleration. Appreciable horizontal temperature gradients set in earlier for smaller thermal conductivity (larger Pr) and for narrower beams. Consequently, the displacement of the maximal velocity should start sooner and be greater for large Pr and for narrower beams; this agrees with the results obtained from the computations. The displacement of the temperature maximum occurs since the gas is heated by the beam with a nonvanishing cross-sectional area; if the gas motion is sufficiently strong

and heat conduction is small, then the amount of heat carried away from the fluid by heat conduction is smaller on the laser beam periphery than the energy of the absorbed radiation, and the temperature of the gas arriving from the axis continues increasing though very slowly. For $Pr = 20$ (Fig. 2) an interesting feature can be seen: Δy_T becomes nonmonotonic on some portion. The displacement of the maximum is greater than that of Δy_T in the other alternatives. The latter takes place since with low heat conduction even very weak heating can exceed the heat loss and the fluid temperature increases due to the absorption in the tail of the Gaussian profile. If there is further rise in q , then a reduction of Δy_T is due to the fact that if the convective motion is strengthened, the role of heat conduction is reduced and also the effect of the Prandtl number appears to be insignificant in the transition to full convection.

3.3. Full Convection. With a further increase in heating the convection also increases. A state of full convection arises which is characterized by the rule

$$V = C_3 q^{1/3}. \quad (15)$$

As predicted in [6], the coefficient in the formula (15) is independent of Pr and it is equal to $C_3 = 0.46$ if one adopts V^* for the characteristic velocity, and it is equal to $C_3 = 0.23$ if $V = V^0$. The lower bound for the full-convection state is higher by 3-4 orders of magnitude than that obtained from the dimensional analysis; in the latter, one sets the convection constants C_N equal to unity [6]. Nevertheless, the bound for this state depends strongly on the ratio of the constants $(C_2/C_3)^6$ and this explains the discrepancy. In this state the flow structure also depends weakly on the determining parameters of the problem. It can be seen in Fig. 1 that a strong jet of hot liquid shoots up from the beam zone and, upon hitting the top of the vessel, forces the hot liquid downward imparting a mushroom shape to the isotherms. Close to the walls a boundary layer develops with high-temperature gradients (associated with a thickening of the isotherms) since the fluid transfers the heat to the walls only by heat conduction (the velocity vanishes at the walls). In the lower part of the vessel numerous secondary eddies arise. The fluid motion is mainly concentrated in the upper portion of the vessel. Obviously, for high q the flow in the vessel must become turbulent; nevertheless, the obtained stationary flows can be regarded as averaged over time if for the coefficients of viscosity and heat conduction one adopts their value for turbulent flows.

In the full-convection state the displacements Δy_V and Δy_T are independent of q as soon as they reach their limiting values: Δy_T is bounded by the beam radius and the increase in Δy_V is hindered by the presence of the flow. In a higher vessel Δy_V can be significantly larger.

Using the results described above of the numerical experiments as a basis one is able to conclude that the dimensional analysis of the Navier-Stokes equation [6] predicts sufficiently well the main features of the photoabsorptive convection. At the same time, the numerical experiments enable one to improve the accuracy of the results and to reveal additional important aspects of convection, for example, the appearance of secondary eddies.

The obtained states differ also as regards the deformation character of the beam in the thermodynamic lens guided by the beam. In Fig. 3 beam trajectories are shown (the deviations of the rays are magnified 100 times) which lie in the axial vertical section of the laser beam passing through the absorbing medium. The ray trajectories were obtained by numerical integration of the equation of the geometrical optics,

$$y'' = \frac{1 + (y')^2}{n(T)} \left[\frac{\partial T}{\partial y} - y' \frac{\partial T}{\partial x} \right] \frac{\partial n}{\partial T}. \quad (16)$$

where $y(x)$ is the ray trajectory; $n(T) = 1 + (n_0 - 1)(T_0/T)$ is the refraction index of the medium. The vertical curve is the principal optical surface of the lens. It can be seen that in the case of weak convection (Fig. 3a) the laser beam only widens, this being accomplished symmetrically relative to the beam axis, which remains a straight line. For full convection (Fig. 3b) the laser beam is distorted without symmetry, the deformation of the beam axis taking place to meet the convective flow. This phenomenon was also observed experimentally [2, 12].

NOTATION

$q = \alpha I_0 L^5 \beta g / \rho_0 c_p v^3$, dimensionless heat emission due to absorption of laser radiation; α , absorption coefficient; I_0 , intensity on the axis of a laser beam; L and H , width and

height of the vessel; T_0 , initial temperature of the medium; ρ_0 , density at $T = T_0$; P , pressure; p , Boussinesq quasipressure; $\chi = k/\rho_0 c_p$, thermal-diffusivity coefficient; k , thermal-conductivity coefficient; ν , kinematic viscosity coefficient; c_p , specific heat at constant pressure; β , heat expansion coefficient; g , gravitational acceleration; $\vec{V} = (V_x, V_y, 0)$, velocity vector; R , universal gas constant; μ , molecular weight; α , laser beam radius; ψ , stream function; ω , vortex; $q_{Re} = (\alpha I_0 a^2 \beta g)/(\rho_0 c_p \nu^3)$, $T_{Re} = [\beta g(T - T_0) \alpha^3]/\nu^2$, $V_{Re} = Va/\nu$, dimensionless quantities with a as the length scale; Pr , Prandtl number; Δy_V , Δy_T , displacement of maxima of velocity or temperature from beam axis; V^* , T^* , ψ^* , maximal values of velocity, temperature and stream function; r , φ , polar coordinates; V^0 , T^0 , values on the ray axis, n , medium refraction index.

LITERATURE CITED

1. J. R. Whinnery et al., IEEE J. Quantum Electron., QE-3, 382 (1967).
2. S. A. Akhmanov, D. P. Krindach, A. V. Migulin, A. P. Sukhorukov, and R. V. Khokhlov, IEEE J. Quantum Electron., QE-4, 568 (1968).
3. D. C. Smith, IEEE J. Quantum Electron., QE-5, 600 (1969).
4. R. A. Chodsko and S. C. Lin, Appl. Phys. Lett., 16, 434 (1970).
5. W. G. Wagner and J. H. Marburger, Opt. Commun., 3, No. 1, 19 (1971).
6. B. P. Gerasimov, V. M. Gordienko, and A. P. Sukhorukov, "Free convection with light absorption," Inst. Probl. Mekh., Preprint No. 59 (1974); Zh. Tekh. Fiz., 45, No. 12 (1975).
7. B. M. Berkovskii and E. F. Nogotov, "Light-absorbing convection in cavities," Inzh.-Fiz. Zh., 19, No. 6 (1970).
8. B. M. Berkovskii and L. P. Ivanov, "Threshold excitement of light-absorbing convection," Mekh. Zhidk. Gaza, No. 3 (1971).
9. B. M. Berkovskii, L. P. Ivanov, and E. F. Nogotov, "Numerical investigation of light-absorbing gravitational convection in closed vessels," in: Convection in Channels [in Russian], ITMO, Minsk (1971).
10. B. P. Gerasimov, "A method for solving problems of convection of incompressible fluids," Inst. Probl. Mekh., Preprint No. 13 (1974).
11. V. A. Aleshkevich, A. V. Migulin, E. P. Orlov, and A. P. Sukhorukov, in: Notes on Reports to the Fifth All-Union Conference on Nonlinear Optics, Kishenev, 1970, Izd. Mosk. Gos. Univ. (1970), p. 56.
12. H. Inaba and H. Ito, IEEE J. Quantum Electron., QE-4, No. 2, 45 (1968).

NONLINEAR STABILITY OF MOTION OF VISCOUS LIQUID BETWEEN CONCENTRIC ROTATING CYLINDERS

E. A. Romashko

UDC 532.527.2

The nonlinear stage of the growth of perturbations in the hypercritical region is investigated in the case of a viscous liquid motion in the gap between two rotating cylinders by using the balance method for perturbation energy.

The stability problem of motion of a viscous liquid in the gap between two rotating cylinders has a special place in the theory of hydrodynamic stability. First, the instability of the rotatory Couette flow is one of the two original types of hydrodynamic instability presented by a simple kind of motion. Second, there are available extensive and sufficiently reliable experimental data for this problem; this is especially important when solving a nonlinear problem since in this case the only test of the authenticity of the theoretical conclusions is their agreement with the experimental results.

The linear stability theory of liquid motion for the system under consideration is well known [1]. We shall not dwell on surveying the literature on this subject but shall only mention that in [2, 3] it was rigorously demonstrated that for suitably high Reynolds numbers the Couette circular motion is unstable. In [4, 5] it was shown that in the linear theory, which is limiting in the sense of the ratio of the radii and the ratio of the cylinder

A. V. Lykov Institute of Heat and Mass Transfer, Academy of Sciences of the Belorussian SSR, Minsk. Translated from Inzhenerno-Fizicheskii Zhurnal, Vol. 33, No. 4, pp. 719-727, October, 1977. Original article submitted April 28, 1976.